# Lawrence Berkeley National Laboratory

**Title**
High Temperature Acclimation of Leaf Gas Exchange, Photochemistry, and Metabolomic Profiles in Populus trichocarpa

**Permalink**
https://escholarship.org/uc/item/6sp1155f

**Authors**
Dewhirst, Rebecca A
Handakumbura, Pubudu
Clendinen, Chaevien S
et al.

# High temperature acclimation of leaf gas exchange, photochemistry, and metabolomic profiles in *Populus trichocarpa*

*Rebecca A. Dewhirst\*[1], Pubudu Handakumbura[2], Chaevien S. Clendinen[2], Eva Arm[2], Kylee Tate[2], Wenzhi Wang[3], Nancy M. Washton[2], Robert P. Young[2], Jenny C. Mortimer[5,6], Nate G. McDowell[3,4], and Kolby J. Jardine[1]*

[1]Climate and Ecosystem Sciences Division, Lawrence Berkeley National Laboratory, Berkeley, CA, 94720, USA

[2]Environmental Molecular Sciences Laboratory, Pacific Northwest National Laboratory, Richland, WA, 99354, USA

[3]Atmospheric Sciences and Global Change Division, Pacific Northwest National Laboratory, PO Box 999, Richland, WA, 99352, USA

[4]School of Biological Sciences, Washington State University, PO Box 644236, Pullman, WA 99164-4236, USA

[5]Joint BioEnergy Institute, Emeryville, CA, 94608, USA

[6]Environmental Genomics and Systems Biology, Biosciences Division, Lawrence Berkeley National Laboratory, Berkeley, CA, 94720, USA

**\*Corresponding author:** Rebecca A Dewhirst: Climate and Ecosystem Sciences Division, Lawrence Berkeley National Laboratory, Berkeley, CA, USA

Email - radewhirst@lbl.gov

## Abstract

High temperatures alter the thermal sensitivities of numerous physiological and biochemical processes that impact tree growth and productivity. Foliar and root applications of methanol have been implicated in plant acclimation to high temperature via the $C_1$ pathway. Here, we characterized temperature acclimation at 35°C of leaf gas exchange, chlorophyll fluorescence and extractable metabolites of potted *Populus trichocarpa* saplings and examined potential influences of mM concentrations of methanol added during soil watering over a two-month period. Relative to plants grown under the low growth temperature (LGT), high growth temperature (HGT) plants showed a suppression of leaf water use and carbon cycling including transpiration (E), net photosynthesis ($P_n$), an estimate of photorespiration ($R_p$), and dark respiration ($R_D$), attributed to reductions in stomatal conductance and direct negative effects on gas exchange and photosynthetic machinery. In contrast, HGT plants showed an upregulation of non-photochemical quenching ($NPQ_t$), the optimum temperature for ETR, and leaf isoprene emissions at 40°C. A large number of metabolites (867) were induced under HGT, many implicated in flavonoid biosynthesis highlighting a potentially protective role for these compounds. Methanol application did not significantly alter leaf gas exchange but slightly reduced the suppression of $R_D$ and $R_p$ by the high growth temperature while slightly impairing ETR, Fv'/Fm', and $q_p$. However, we were unable to determine if soil methanol was sufficiently taken up by the plant to have a direct effect on foliar processes. A small number of extracted leaf tissue metabolites (55 out of 10,015) showed significantly altered abundances under LGT and methanol treatments relative to water controls, and this increased in compound number (222) at the HGT. The results demonstrate the large physiological and biochemical impacts of high growth temperature on poplar seedlings and highlights the enhancement of the optimum temperature of ETR as a rapid thermal acclimation mechanism. Although no large effect on leaf physiology was observed, the results are consistent with methanol both impairing photochemistry of the light reactions via formaldehyde toxicity, and stimulating photosynthesis and dark respiration through formate oxidation to $CO_2$.

# 1. <u>Introduction</u>

Global ecosystems are experiencing an unprecedented upward trend in surface temperature that strongly enhances leaf-to-atmosphere vapor pressure deficits, a key driver of plant transpiration (E)[1]. While stomatal conductance ($g_s$) and net photosynthesis ($P_n$), can be stimulated by warming, high temperatures beyond the species or environmental optimal values are associated with suppressions in $g_s$ and $P_n$[2]. This stomatal behavior helps to avoid excessive water loss and xylem hydraulic failure, a major potential mechanism of tree mortality[3]. Although increasing surface temperatures between 1982 and 1999 were associated with a global upward trend of net primary productivity (NPP), the past decade has been the warmest on record with high temperature anomalies correlated with reductions in global NPP[4]. In addition, decreases in biomass gains, widespread insect epidemics, increased vegetation mortality, and shortening of carbon residence times have been linked to high surface warming anomalies in numerous ecosystems[5,6]. Therefore, understanding the underlying biochemical and physiological processes involved in tree response and acclimation to elevated surface temperatures are critical for accurately predicting functions, properties, and structures of natural and managed ecosystems exposed to surface warming. This knowledge is particularly valuable for dedicated bioenergy and biomaterial feedstock crops, such as the fast-growing tree species *Populus trichocarpa*. An annotated whole genome sequence for *P. trichocarpa* was first released in 2004[7], enabling the potential for engineering improved resilience to warming using plant synthetic biology[8].

As instantaneous leaf temperatures increase in $C_3$ plants, photorespiration rates rise faster than photosynthetic rates leading to an increase in the ratio of photorespiratory production of $CO_2$ to photosynthetic $CO_2$ assimilation[9]. This differential temperature sensitivity of photosynthesis ($CO_2$ sink) and photorespiration ($CO_2$ source) strongly influences the temperature response curves of net photosynthesis ($P_n$), which typically shows a clear temperature optimum, above which $P_n$ declines[10]. However, previous research has shown that temperature acclimation to prolonged high temperatures in many species can result in a slight increase in the optimum temperature of $P_n$ across species[11]. Acclimation of photosynthetic rates to high temperature was detected as an increase in the maximum rate of photosynthetic electron transport ($J_{max}$) and the maximum rate of rubisco carboxylation ($V_{cmax}$)[12]. With changes in growth temperature, many plants show phenotypic plasticity in their photosynthetic properties with plants grown at higher temperatures shifting their optimal temperature of $P_n$ to higher values[13]. However, this is often difficult to detect as an analysis of 103 species showed that constructive adjustment of the optimal temperature of $P_n$ were only reported in half of the species[14]. Likewise, field observations of sites in Panama could not detect a higher temperature optimum of photosynthesis ($T_{Opt}$) in fast growing pioneer species with light-demanding high photosynthetic capacity versus shade-tolerant species with lower photosynthetic capacity[15].

Moreover, the response of stomatal conductance ($g_s$) to changes in growth temperature strongly impacts the temperature response of $P_n$ [16], but this behavior can be uncoupled from the photochemical phase of photosynthesis. For example, in the 'hyperthermophile' early successional species *Vismia guianensis* in the central Amazon, electron transport rates (ETR) increased with temperature in concert with

isoprene emissions (a primary product of photosynthesis), even as reductions in $g_s$ constrained $P_n$[17]. However, the magnitude and direction of $g_s$ acclimation to temperature  is inconsistent across species and conditions, with higher growth temperatures enhancing $g_s$ in the thermophilic tree *Zizphus spinachristi*[18] while $g_s$ suppression under higher growth temperatures was reported in *Ulmus americana*[19] and *Populus x euramericana*[20]. Heat waves coupled with drought further suppressed $g_s$ in *Robinia pseudoacacia* and *Pseudotsuga menziesii*[21].

In addition to changes in leaf gas exchange parameters, leaf metabolite profiles are also altered during heat stress, in part controlled by heat stress transcription factors[22]. TCA (tricarboxylic acid) cycle intermediates decreased at high growth temperature in potato leaves and tubers[23] and *Arabidopsis* leaves[24]. Secondary metabolites have also been implicated in the heat stress response, for instance terpenoid emissions increased upon heat stress in the medicinal herb *Achillea millefolium*[25], and the abundance of several phytosterols in potato were increased at high growth temperature[23]. However, the expression of genes involved in secondary metabolite biosynthesis in hop (*Humulus lupulus*) leaves were reduced under heat stress[26]. Genes involved in flavonoid and anthocyanin biosynthesis were down-regulated under severe heat stress but up-regulated during moderate heat stress in tea (*Camellia sinensis*)[27], highlighting that these metabolomic responses are nuanced and complex. However, little is known about the response to heat stress of poplar metabolic profiles.

In this study on temperature acclimation of leaf gas exchange in *P. trichocarpa* saplings, we hypothesize (**H1**) that $g_s$ is down regulated at high growth temperatures and this will lead to a suppression in E and $P_n$ as well as dark respiration ($R_d$). However, the optimum temperature of ETR will be stimulated as

well as the emissions of isoprene through the utilization of products of the light reactions[17]. Moreover, downstream pathways involved in secondary metabolite biosynthesis will also alter under HGT.

Increases in tropospheric $CO_2$ concentrations partially counteract the negative effects of high temperature on $P_n$ by enhancing the ratio of photosynthetic carbon gains to photorespiratory production of $CO_2$[28]. In addition to atmospheric $CO_2$, the potential for temperature-stimulated internal sources of $CO_2$ from within the leaf to also enhance this ratio have been considered[29]. For example, over 50 years ago, the existence of an oxidative $C_1$ pathway (methanol, formaldehyde, formic acid, and $CO_2$) was demonstrated in $C_3$ plants and shown to contribute to $CO_2$ assimilated by photosynthesis as well as to contribute to the production of photorespiratory intermediates, like serine[30]. Thought to be initiated by the release of methanol from the hydrolysis of methylated pectin of primary cell walls[31], the reservoir and flux of carbon through the $C_1$ pathway in plants remains largely unquantified. However, the degree of pectin methylation has been shown to be highly species-dependent with a wide range of values reported (10-70%)[32]. While many volatiles emitted into the atmosphere by plants are highly species-specific (e.g. volatile isoprenoids), high plant methanol emissions have been consistently observed from managed and natural terrestrial ecosystems[33] with plant-derived methanol recognized as the most abundant non-methane volatile organic compound in the atmosphere[34].

^{13}C-NMR studies of [^{13}C]formaldehyde metabolism by *Arabidopsis thaliana* seedlings demonstrated that formaldehyde integrates into photorespiration via the universal $C_1$ donor $CH_2$-THF forming serine in mitochondria independent from the re-

assimilation of formate-derived $CO_2$ in chloroplasts[35]. Dynamic pulse-chase labeling experiments using solutions of [$^{13}$C]methanol and [$^{13}$C]formaldehyde delivered via the transpiration stream demonstrated a rapid turnover of $C_1$ pathway intermediates (minutes) in physiologically active branches of the tropical tree species *Inga edulis*[36]. While fast interconversion between [$^{13}$C]methanol and [$^{13}$C]formaldehyde was observed upon labeling with [$^{13}$C]methanol or [$^{13}$C]formaldehyde, delivery of [$^{13}$C]formate resulted in emissions of [$^{13}$C]$CO_2$ without emissions of [$^{13}$C]methanol or [$^{13}$C]formaldehyde. This demonstrated the $C_1$ intermediate, formate, as an irreversible commitment to $CO_2$ production in chloroplasts. However, the quantitative importance of the $C_1$ pathway for central carbon metabolism is unknown, including during high temperature stress where its activity is expected to accelerate. This uncertainty is partly due to the fact that the intermediates of the $C_1$ pathway are difficult to measure due to their high volatility (methanol, formaldehyde, formic acid) and reactivity (formaldehyde). Nonetheless, there may be an important role of methanol in enhancing biomass accumulation rates in crops under abiotic stress through a proposed mechanism involving photorespiratory production of serine and $CO_2$ production in chloroplasts[37]. For example, high concentration methanol solutions (% vol/vol) regularly sprayed onto the foliage of $C_3$ plants experiencing environmental stress, enhanced plant productivity, but not in $C_4$ plants[38]. While some of the subsequent studies also observed a stimulation of biomass gains from foliar methanol sprays[39], some did not, including an extensive field test[40] where severe toxic effects were observed when very high aqueous concentrations of methanol were delivered to roots (e.g. 40-80%).

Taken together, the results led us to hypothesize (**H2**) an important metabolic role of the methanol-initiated $C_1$ pathway during high temperature stress in $C_3$ plants. Specifically, we hypothesize that for *P. trichocarpa* saplings grown at a high growth temperature, methanol-treated plants will show increased thermotolerance of photosynthesis displayed by higher rates of $P_n$ and photochemical parameters of the light reactions including ETR, Fv'/Fm', and $q_p$. Moreover, due to $CO_2$ production via the $C_1$ pathway, methanol-treated plants are also anticipated to have suppressed rates of photorespiration ($R_p$) and enhanced rates of dark respiration ($R_D$). Finally, methanol-treated plants are predicted to have higher leaf concentrations of photosynthetic products including sugars, fatty acids, isoprenoids, etc. In order to evaluate **H1** and **H2**, we characterized leaf gas exchange, photochemical parameters of photosynthesis, and extractable metabolite responses to high growth temperature (HGT, 35°C) and the effect of mM concentrations of methanol solutions (0, 9, and 27 mM) delivered to the soil of potted *P. trichocarpa* saplings over eight weeks. These concentrations were chosen due to the likely presence of microbial methanol assimilation in the soil, and previous observations that 10 mM methanol is rapidly metabolized in physiologically active tree branches[41].

## 2. **Experimental section**

### *2.1 Plant materials and growth conditions*

36 *Populus trichocarpa* trees in 1-gallon pots (6.5" diameter and 7" deep) with Sunshine MVP soil mix (Sun Gro Horticulture, MA, USA) and between 3.0-3.5' in height were obtained from an established tree nursery in Eastern Washington, USA (Plants of the Wild). The trees were delivered to the Environmental Molecular

Sciences Laboratory (EMSL) on 03 June 2019 and placed in two identical growth chambers (Percival Intellus Control System, Iowa, USA) maintained under a 16-hour photoperiod (6:00-22:00) with constant daytime photosynthetically active radiation intensity of (350 μmol m$^{-2}$s$^{-1}$), and day/night air temperatures of 25°C/20°C and a constant relative humidity set at 60%. All plants were watered with 50 mL of reverse osmosis water on arrival. Following a two-day equilibration time, half of the trees (18) in the first growth chamber were maintained under the normal daytime air temperature conditions of (25°C) while the other 18 trees in the second growth chamber were exposed to an increased daytime air temperature of (35°C) on 05 June 2019. Plants were watered with 50 mL of water or one of the three methanol solutions (0, 9 or 27 mM) for the first two days (06 June and 07 June), then watered with 200 mL water or methanol solutions every other day until the end of the experiment on 01 Aug 2019 (total experimental duration of 57 days). These methanol concentrations were chosen to be physiologically relevant, but low enough to avoid methanol toxicity. A summary timeline of the leaf gas exchange, chlorophyll fluorescence, and metabolomics data collected including biological replicates is shown in **Table 1**.

**Table 1 – Timeline of measurements (June 2019 – July 2019)**

| Measurements | Values (approximate dates) |
|---|---|
| Watering/methanol addition | 36 repeated throughout June and July (daily) |
| Licor6800 - dark adapted leaf gas exchange and fluorescence | 35 (Jun 11); 35 (Jul 8); 36 (Jul 17); 30 (Jul 25) |
| Licor6800 - light adapted leaf gas exchange and flouresence in air under standard conditions | 17 (Jun 11); 30 (Jun 18); 27 (Jun 25); 27 (Jul 1); 36 (Jul 9); 12 (Jul 17); 22  13 (Jul 30–31) |
| Licor6800 - light adapted leaf gas exchange and flouresence in nitrogen under standard conditions | 18 (Jun 11); 36 (Jul 9); 22  13 (Jul 30–31) |
| Licor6800 - temperature response curves | 8  10 (Jul 10–11); 6 (Aug 1) |
| Handheld flourometer - measurement of NPQt | 36 (Jun 11); 36 (Jun 18); 36 (Jun 24); 36 (Jul 1); 36 (Jul 9); 36 (Jul 16); 19 (Jul 23); 36 (Jul 30) |
| Metabolomics - leaf removed for LC-MS analysis | 36 (Jun 11); 36 (Jun 18); 36 (Jun 24); 36 (Jul 1); 36 (Jul 9); 36 (Jul 16); 36 (Jul 24) |
| Isoprene emissions - gas sample collected at leaf temperature of 45°c for PTR-MS analysis | 18 (Jul 10) |

**Table 1**: Timeline of experimental treatments, observations, and biological replicates throughout the 2 month (57 day) experimental period on 36 poplar saplings. The numbers refer to the total number of individuals analyzed at each timepoint.

## 2.2 Leaf gas exchange

A portable photosynthesis system (6800, LI-COR Biosciences, Nebraska, USA) was used to collect leaf gas exchange fluxes with gas flow rate entering the 6 cm$^2$ leaf chamber maintained at 500 µmol s$^{-1}$, and a reference $CO_2$ and $H_2O$ concentrations of 400 ppm and 25 mmol mol$^{-1}$, respectively. For measurements under standard environmental conditions, leaf temperature was maintained at 30°C with measurements in the light with a PAR of 1000 µmol m$^{-2}$ s$^{-1}$ (color spectrum r90B40, 960 µmol m$^{-2}$ s$^{-1}$ red, 40 µmol m$^{-2}$ s$^{-1}$ blue) and dark measurements with a PAR of 0 µmol m$^{-2}$ s$^{-1}$. Following gas exchange measurements in the light under air, with the leaf still in the enclosure, the air source was replaced with nitrogen gas (while

maintaining 400 ppm reference $CO_2$) using an external cylinder to block photorespiration and mitochondrial (dark) respiration. Gas exchange measurements were logged after 1 minute of leaf exposure to the nitrogen atmosphere. Mean leaf photorespiration rates in the light for each of the experimental treatments were estimated by subtracting the mean values of $P_n$(air) from $P_n$($N_2$). Finally, leaf gas-exchange temperature response curves were collected in the light (PAR of 1000 $\mu mol\ m^{-2}\ s^{-1}$) for a subset of individuals with leaf temperatures increasing from 25°C to 40°C by 2.5°C increments.

For all leaf gas exchange measurements, each plant was removed individually from the growth chamber and measurements initiated within 3 minutes, following which it was returned to the growth chamber. Where possible, mature leaves near the top of each branch were studied. After placing the leaf in the chamber, gas exchange measurements were collected after an equilibration period of 3-10 minutes in the light and 2-3 minutes in the dark, in order to allow $P_n$ and $g_s$ to reach steady state conditions. Dark measurements were collected after dark adapting the leaf for 20 minutes using aluminum foil just prior to measurements.

### 2.3 Chlorophyll fluorescence

For each of the three gas exchange experiments using the Li6800 photosynthesis system (light, dark, and temperature responses curves), chlorophyll fluorescence measurements were simultaneously collected using a multiphase flash fluorometer (6800-01F, LI-COR Biosciences, USA). Following leaf acclimation to each environmental condition (see section 4.2), an actinic saturating light pulse (color spectrum r90B40, 8,000 $\mu mol\ m^{-2}\ s^{-1}$ red light/40 $\mu mol\ m^{-2}\ s^{-1}$ blue light) was applied for 1,000 ms with a dark modulation rate of 50 Hz, light modulation rate of 1 kHz),

flash modulation rate of 250 kHz, and 15 sec chlorophyll fluorescence signal averaging (100 Hz data output rate with a margin of 5 points before and after flash).

The average chlorophyll fluorescence signal was used to determine minimum fluorescence (Fo), maximum fluorescence (Fm), and steady-state fluorescence (Fs). Derived photochemical parameters were calculated according to **Eqs. 1-3** where derived parameters with prime, for example Fo', are values related to the data in the light and those with no prime corresponding to data from the dark-adapted leaf. Derived photochemical parameters were calculated including photosynthetic electron transport (ETR, µmol e⁻ m⁻² s⁻¹), maximum quantum efficiency of PSII in the dark ($\frac{Fv}{Fm}$) and light ($\frac{Fv'}{Fm'}$), and photochemical quenching ($q_p$) as follows[42]:

**Eq. 1.** $ETR = \left(\frac{Fm'-Fs}{Fm'}\right) \cdot f \cdot PAR \cdot \alpha\, leaf$, where $f$ is the fraction of the quantum absorbed and used by Photosystem II, with a value of 0.5 used for $C_3$ plants[43], PAR is incident photon flux density, and $\alpha_{leaf}$ is leaf absorbance (0.87).

**Eq. 2.** In the dark $\frac{Fv}{Fm} = \frac{Fm-Fo}{Fm}$ and in the light $\frac{Fv'}{Fm'} = \frac{Fm'-Fo'}{Fm'}$

**Eq. 3.** $q_p = \frac{Fm'-F'}{Fm'-Fo'}$

### 2.4 Liquid chromatography mass spectrometry (LC-MS):

Throughout the experiment, one leaf per tree was removed every week and immediately flash frozen in liquid $N_2$ and ground using a ball mill, lyophilized, and stored at -80°C before being analyzed for metabolites. Metabolites were extracted

from 40 mg of lyophilized samples in 1 mL of methanol: water (80:20) and centrifuged at 1,200 rpm for 1 hour at 21°C followed by 4,000 rpm for 10 min.

Supernatants were collected for metabolite analyses using a benchtop LC-MS/MS. Samples were randomized and analyzed using an Ultimate 3000 HPLC system (Thermo Fisher Scientific/Dionex RSLC, Dionex, Massachusetts, USA) LC system coupled to an LTQ Orbitrap Velos high-resolution mass spectrometer (Thermo Fisher Scientific, Massachusetts, USA) equipped with a HESI (heated electrospray ionization, Thermo Fisher Scientific). The mass spectrometer operated in FTMS (Fourier Transform Mass Spectrometry) full-scan mode with high-mass resolution (60,000) and mass range acquisition of 70–800 m/z. Samples were analyzed in both positive (+ve) and negative (−ve) ionization modes. Data dependent acquisition (DDA) resulted in low-resolution MS2 on the top 10 ions in each scan. Compounds were separated using a reversed-phase C18 Hypersil gold column (150 × 2.1 mm, 3 µm particle size; Thermo Scientific, Waltham, MA, USA) with a column temperature of 30°C at a flow rate of 300 µL min$^{-1}$. Mobile phase A (0.1% acetic acid) and mobile phase B (acetonitrile) were initially at a ratio of 90:10 respectively and maintained for 5 min. The mobile phase continued in with the following gradients: transition linearly to 10% mobile phase A between 5-20 min; maintain 10% A between 20-22 min; recover to 90% A between 22-25 min. After each sample the column was washed and stabilized for 10 min. A QC standard mixture was injected about every 20 samples and an experimental blank (80:20 H2O: MeOH) samples were injected every 10 samples.

All the data were aligned, peaks selected, and de-isotoped using MZmine [44]. LC-MS data was analyzed and visualized with metaboanalyst [45] and R version 4.0.0.

Identified compounds were assigned to a metabolic pathway group using KEGG database (https://www.genome.jp/kegg/pathway.html).

## 2.5 Leaf isoprene emissions and NPQ$_t$

During the mid-point in the experiment (10-11 August 2020), leaf isoprene emission analysis was collected from 3 LGT individuals and 3 HGT individuals at leaf temperature of 40°C. 30 ml air samples were collected from the auxiliary air sample port of the LI6800 photosynthesis system with an illuminated leaf in the chamber in 20-30 seconds manually using a syringe and analyzed for isoprene concentrations using proton transfer reaction mass spectrometry (PTR-MS, Ionicon, Austria, with a QMZ 422 quadrupole, Balzers, Switzerland). 3 samples were also collected from an empty chamber (no leaf) in order to subtract any background signal. The PTR-MS was operated with a drift tube voltage of 600 V and pressure of 1.9 mb. The following mass to charge (m/z) ratios were monitored: m/z 32 ($O_2^+$), m/z 21 ($H_3^{18}O$), m/z 37 ($H_2O$-$H_3O^+$), and m/z 69 (protonated isoprene: $H^+$-$C_5H_8$).

In addition, throughout the experiment, a MultispecQ handheld fluorometer was used to determine the non-photochemical quenching (NPQ$_t$) parameter in the light according to **Eq. 4**[46]. A comparable leaf with similar distance to the growth chamber light source was marked from each plant and the fluorescence was captured weekly during the same time of the diurnal cycle. The sensor head was installed on each leaf directly within the enclosure without removing the plant from the growth chamber. Measurements lasting roughly 1 min each were acquired from each individual linked to the PhotosynQ network (https://photosynq.org) via Bluetooth connection to a smartphone.

**Eq. 4.** $NPQ_t = \dfrac{4.88}{\dfrac{Fm'}{Fo'} - 1} - 1$

## 2.6 Statistical analysis

ANOVA and Tukey post hoc tests were carried out in R version 4.0.0 to determine significant effects of temperature and methanol treatment on leaf gas exchange variables. Data was categorized by methanol concentration (0 - 27 mM) at each temperature (LGT or HGT) resulting in 6 groups each comprising 6 individual trees. The number of observations included in the statistical analysis differed with each variable and group (see **Table 2**). All statistically significant results (p ≤0.05) are reported with the exact p value, unless p< 0.0001 (**Table 3**), and originate from ANOVA with Tukey post hoc analysis. LC-MS data was analyzed and visualized with metaboanalyst and R version 4.0.0. Compounds were considered significantly altered by either temperature of methanol treatment if they showed a ∓ 2-fold change in abundance which was statistically significant (p≤0.05, Students t-test).

| Growth Temp/Methanol | A, $g_s$, E, $F_v'/F_m'$, ETR, $q_p$ | Isoprene | $NPQ_t$ | $T_{opt}$ETR | $R_d$ | $R_p$ |
|---|---|---|---|---|---|---|
| LGT (0 mM) | 38 | 3 | 49 | 4 | 24 | 16 |
| LGT (9 mM) | 29 | 3 | 49 | 2 | 23 | 15 |
| LGT (27 mM) | 29 | 3 | 47 | 3 | 23 | 16 |
| HGT (0 mM) | 32 | 3 | 45 | 2 | 17 | 14 |
| HGT (9 mM) | 31 | 3 | 43 | 3 | 23 | 15 |

| HGT (27 mM) | 24 | 3 | 42 | 3 | 22 | 13 |
|---|---|---|---|---|---|---|

**Table 2**: Number of leaf observations for each variable shown used to calculate the mean values in Figures. 1-4.

| Temperature | 25°C v 35°C | 25°C v 35°C | 25°C v 35°C | 25°C | 25°C | 25°C | 35°C | 35°C | 35°C |
| Methanol | 0mM | 9mM | 27mM | 0mM v 9mM | 0mM v 27mM | 9mM v 27mM | 0mM v 9mM | 0mM v 27mM | 9mM v 27mM |
|---|---|---|---|---|---|---|---|---|---|
| Net photosynthesis | <0.0001 | 0.0048 | 0.0035 | 0.1516 | 0.5736 | 0.9763 | 0.7970 | 0.9674 | 0.9988 |
| Transpiration | <0.0001 | 0.0350 | 0.0074 | 0.0015 | 0.0390 | 0.9378 | 0.6011 | 0.7896 | 1.0000 |
| Stomatal conductance | <0.0001 | 0.0406 | 0.0169 | 0.0003 | 0.0047 | 0.9813 | 0.6618 | 0.8286 | 1.0000 |
| Photosynthetic electron transport | <0.0001 | 0.0001 | <0.0001 | 0.8604 | 1.0000 | 0.9763 | 0.9808 | 0.9979 | 0.9999 |
| Maximum quantum yield of PSII | <0.0001 | 0.0406 | 0.0169 | 0.0003 | 0.0047 | 0.9813 | 0.6618 | 0.8286 | 1.0000 |
| Photochemical quenching | <0.0001 | 0.0001 | <0.0001 | 0.8604 | 1.0000 | 0.8921 | 0.9808 | 0.9979 | 0.9999 |
| Leaf respiration | 0.0001 | 0.0154 | 0.0053 | 0.8630 | 0.9968 | 0.9856 | 0.9979 | 0.9812 | 0.9997 |
| Photorespiration | 0.4650 | 0.8777 | 0.9952 | 1.0000 | 0.9971 | 0.9915 | 0.9631 | 0.9695 | 1.0000 |
| NPQt | 0.0002 | 0.1067 | <0.0001 | 0.2273 | 0.9987 | 0.4598 | 0.9997 | 0.8748 | 0.9656 |
| Isoprene emissions | 0.6000 | 0.3800 | 0.6000 | 0.6000 | 0.6000 | 0.7500 | 0.7500 | 1.0000 | 0.7500 |

**Table 3:** P values of ANOVA and Tukey post-hoc analysis. Statistically significant values are in bold. Data was compared between temperatures (at the same methanol concentration, the first three columns of values) and between methanol concentrations (at the same temperature, the last six columns of values).

## 3. Results

### 3.1 Impacts of HGT on leaf gas exchange and photochemical parameters of photosynthesis

After arrival at the Environmental Molecular Sciences Laboratory (EMSL) in eastern Washington, USA, the 36 poplar saplings were placed within plant growth chambers (18 in LGT and 18 in HGT) and allowed five days to acclimate prior to the

commencement of leaf measurements, which started on day 6 and continued periodically until day 57 (**Table 1**). In order to facilitate the comparison of gas exchange between LGT and HGT plants, measurements were conducted on leaves held at 30°C. To determine temperature acclimation response of the poplar saplings we first consider only the 0 mM methanol data. Consistent with hypothesis **H1**, plants grown in 0 mM methanol at HGT showed considerable downward acclimation of leaf water use and carbon cycling, relative to plants grown in 0 mM methanol at LGT. For example, relative to LGT plants, mean gas exchange fluxes under constant leaf temperature and light intensity from the HGT plants showed a strong decrease in leaf transpiration (E; decrease of 54.8%, p<0.0001, ANOVA, LGT n=38, HGT n=32; **Table 2 and 3**) and net photosynthesis ($P_n$; decrease of 50.6%, p<0.0001) associated with a down regulation in stomatal conductance ($g_s$; decrease of 61.0%; p<0.0001; ANOVA, LGT n=38, HGT n=32, **Figure 1**). Moreover, coupled gas exchange and chlorophyll fluorescence observations detected a significant suppression in HGT plants of several photochemical parameters of photosynthesis including electron transport rates (ETR; 44.1% decrease, p<0.0001, ANOVA, LGT n=38, HGT n=32), quantum yield of PSII in the light (Fv'/Fm'; 44.1% decrease, p<0.0001, ANOVA, LGT n=38, HGT n=32), and photochemical quenching ($q_p$, 44.1%, p<0.0001; **Figure 2,** ANOVA, LGT n=38, HGT n=32). Fv/Fm measurements reveal increased stress in the HGT plants compared to the LGT plants (**Figure 3a**). Leaf gas exchange measurements on dark adapted leaves also revealed a suppression of dark respiration rates in HGT plants ($R_D$; 36.8% decrease, p=0.0001, LGT n=24, HGT n=17), and estimates of photorespiration in the light using a nitrogen atmosphere were severely suppressed in the HGT plants ($R_P$, 93.8%

decrease, p= n/s, LGT n=16, HGT n=14), such that little stimulation of $P_n$ occurred under nitrogen (**Figure 3**).
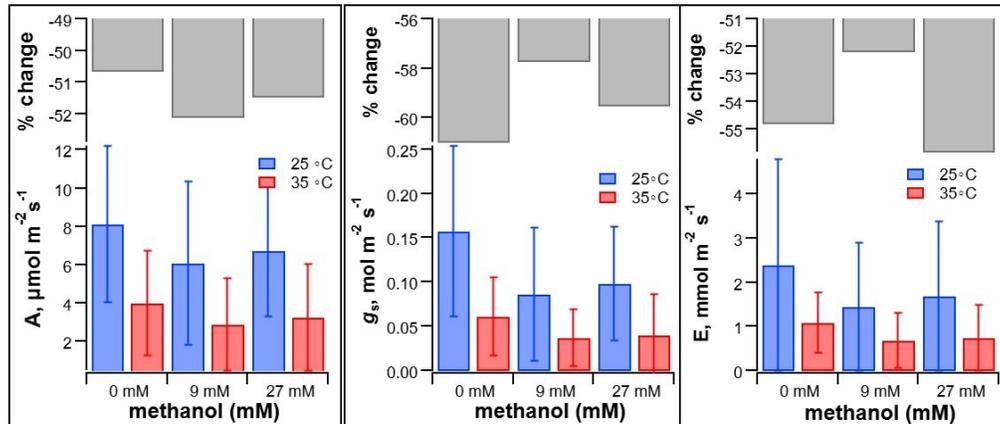


**Figure 1**: Mean values +/- 1 standard deviation of leaf net photosynthesis ($P_n$), stomatal conductance ($g_s$), and transpiration (E) determined over the two-month experimental period in 2019 by a Li6800 photosynthesis system under two growth temperatures (25 °C, LGT and 35 °C, HGT) and three methanol concentrations (0, 9, and 27 mM).
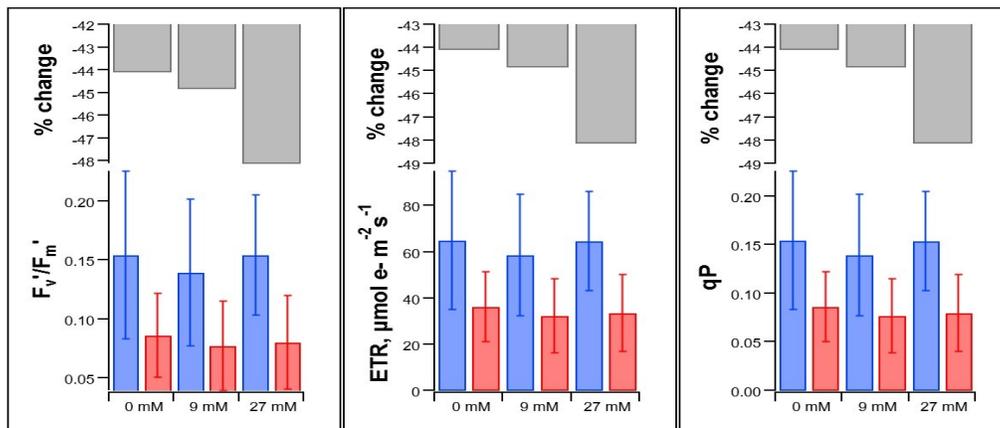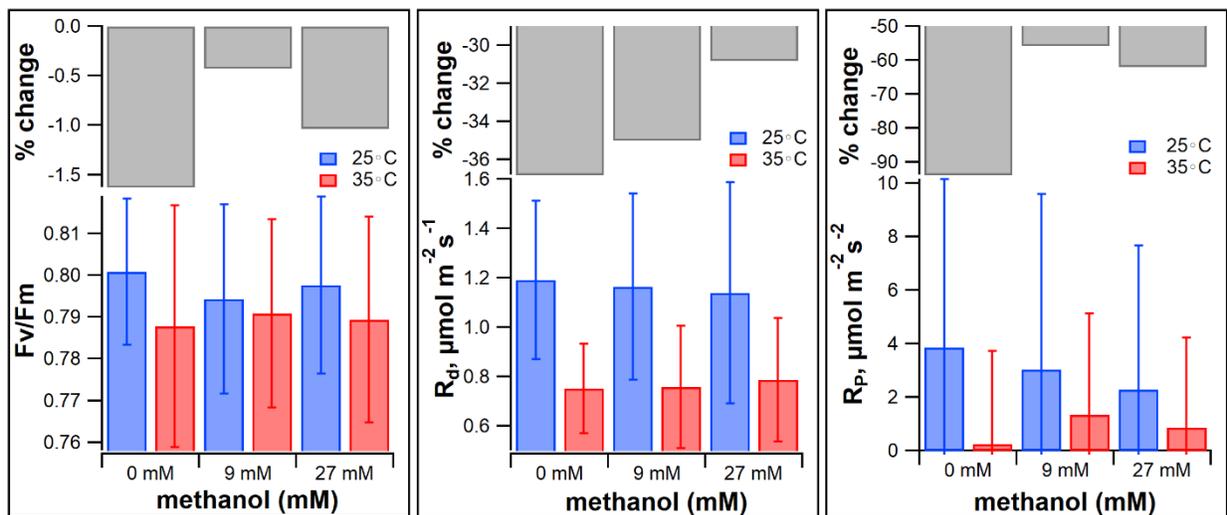
**Figure 2:** Mean values +/- 1 standard deviation of maximum quantum yield of PSII (Fv'/Fm') in the light, photosynthetic electron transport (ETR), and photochemical quenching ($q_p$) determined over the two-month experimental period in 2019 by a Li6800 photosynthesis system under two growth temperatures (25 °C, LGT and 35 °C, HGT) and three methanol concentrations (0, 9, and 27 mM).



**Figure 3**: Mean values +/- 1 standard deviation of maximum potential quantum efficiency of Photosystem II (Fv/ Fm) leaf respiration ($R_d$) and photorespiration ($R_p$) determined over the two-month experimental period in 2019 by a Li6800 photosynthesis system under two growth temperatures (25 °C, LGT and 35 °C, HGT) and three methanol concentrations (0, 9, and 27 mM).

During a single set of measurements, isoprene emissions were quantified at a leaf temperature of 40°C with HGT plants showing higher values relative to LGT plants at 0 mM methanol (**Figure 4a)**, but this difference was not statistically

significant (28.6% increase, p=0.6, LGT n=3, HGT n=3), likely due to the low sample number (n=3 for LGT and HGT). NPQt, a chlorophyll fluorescence parameter for estimation of non-photochemical quenching of excitons in photosystem-II-associated antenna complexes[46] was determined using a handheld fluorimeter. In water control plants (0 mM methanol), NPQt significantly increased under HGT conditions compared to LGT conditions (74.3% increase, p=0.0002, LGT n=49, HGT n=45; **Figure 4b**), consistent with the observed reduction in Fv'/Fm' (**Figure 2a**). Moreover, despite showing lower magnitudes under standard environmental conditions, (**Figure 2b**), the optimum temperature of ETR was found to be enhanced in HGT plants relative to LGT plants regardless of methanol treatment. Leaf temperature response curves revealed that HGT plants showed significant upward acclimation of the optimum temperature (LGT: 35.7°C versus HGT: 38.7°C; **Figure 5c**), representing a 3.0°C increase (8.3% increase p<0.0001, LGT n=12, HGT n=10).
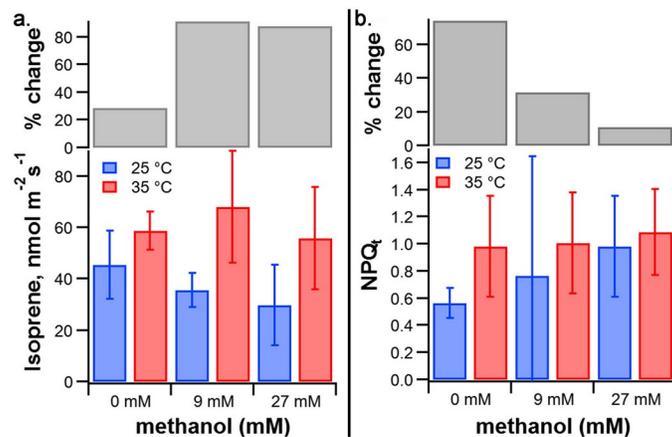


**Figure 4:** Mean values +/- 1 standard deviation in the light of isoprene emissions at 40 °C leaf temperature determined by PTR-MS (LGT: n=3, HGT: n=3) and NPQt determined by a handheld fluorometer (LGT: n=49, HGT: n=45) under two growth

temperatures (25°C and 35°C) and three methanol treatments (0 mM, 9 mM, and 27 mM).
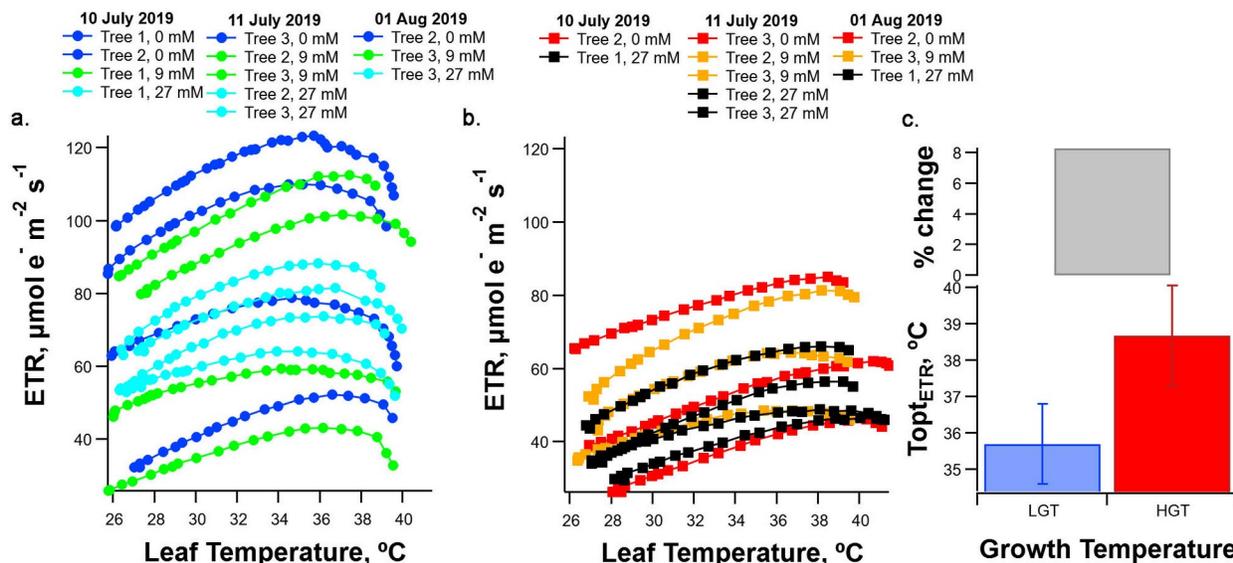


**Figure 5**: Leaf temperature ETR response curves in the light during three different dates for **a**) LGT plants (n=12) and **b**) HGT plants (n=10). Note, select plants from each of the three methanol treatments were measured (0 mM, 9 mM, and 27 mM). Also shown **c**) are the mean optimum leaf temperature of ETR (Topt$_{ETR}$) +/- 1 standard deviation for the LGT and HGT plants shown in **a**. and **b**.

## 3.2 Impacts of HGT on extractable LC-MS/MS metabolites

Non-targeted LC-MS/MS analysis of leaf metabolites extracted in methanol: water (80:20) detected 10,015 features from leaf samples collected weekly throughout the experiment from each individual (each feature represented by a single m/z value). Of these metabolites, 867 showed significant changes in abundance in HGT relative to LGT samples (**Figure 6; supplementary table 1**), as

defined by a greater than 2-fold difference and p ≤ 0.05 (t-test). 490 metabolites decreased under HGT and 377 increased in abundance under HGT. Putative compound identification based on MS/MS mass spectral comparisons with known compounds were obtained for 110 of these 867 significant metabolites (**supplementary table 1**) and grouped according to their relevant metabolic activities as defined by the Kyoto Encyclopedia of Genes and Genomes (KEGG, https://www.genome.jp/kegg/pathway.html). The majority of the identified extractable metabolites are involved in secondary metabolism, predominantly the flavonoid and polyphenolic pathways (the latter included in 'other secondary metabolites' KEGG category; **Table 4**). Within the flavonoid biosynthetic pathway, 20 metabolites were decreased under HGT and 10 increased. This pattern was repeated with other secondary metabolites, with 30 compounds decreasing under HGT and 16 increasing. For example, 5 compounds within the terpenoid class of secondary metabolites were identified in this analysis, with two decreasing in abundance under HGT and three increasing. Identified metabolites involved in lipid biosynthesis generally decreased under HGT, whereas those involved in amino acid and carbohydrate pathways increased under HGT (**Table 4**).
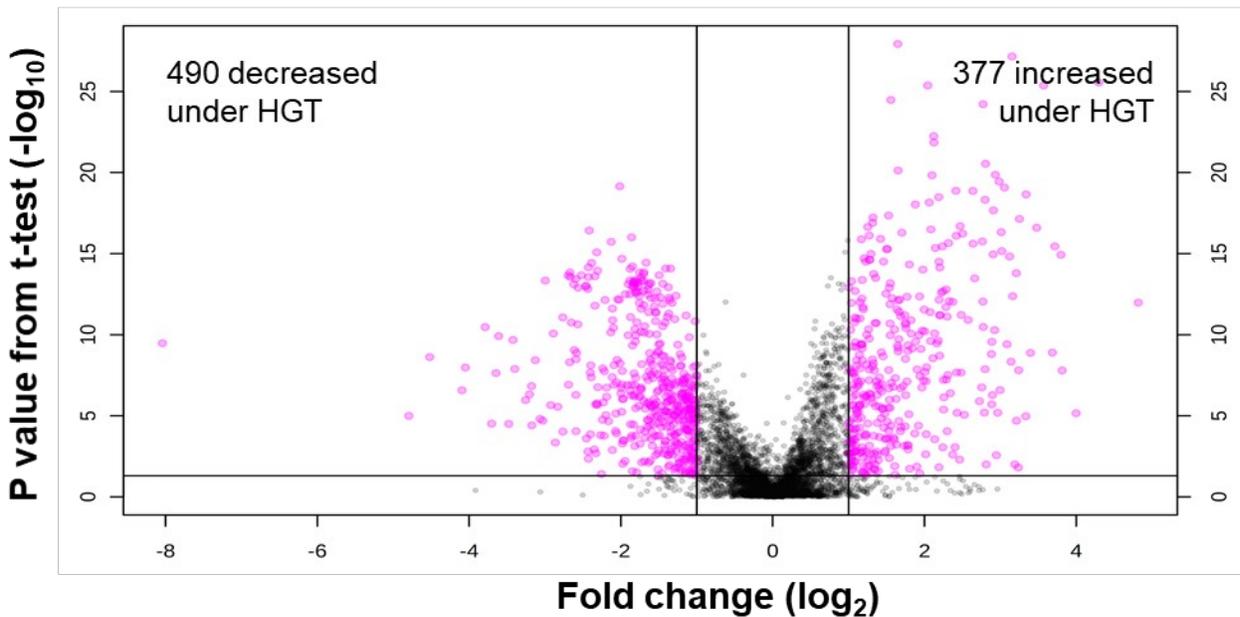
**Figure 6**: Volcano plot showing growth temperature-induced differences in extracted leaf compound abundances (LC-MS positive mode). Compounds that have a greater than ± 2-fold abundance change (x-axis) that is statistically significant (p<0.05, t-test; y axis) between LGT and HGT plants at 0 mM methanol are shown in pink. The number of significant compounds that decreased in abundance in the HGT plants relative to LGT plants is indicated on the left side of the plot, and the number of compounds significantly increased in the HGT plants relative to LGT plants is indicated on the right side.

|  | HGT effect (0 mM meOH) | |
|---|---|---|
|  | Decrease | Increased |

| | d | |
|---|---|---|
| Amino acid | 2 | 7 |
| Carbohydrates | 1 | 6 |
| Lipids | 12 | 1 |
| Flavonoids | 20 | 10 |
| Terpenoids | 2 | 3 |
| Other secondary metabolites | 30 | 16 |

**Table 4:** Summary of HGT effect on metabolomic profiles. The number of samples that it was possible to obtain a compound ID for that decreased or increased in each metabolic pathway as defined by KEGG under HGT are indicated. All compounds included in this analysis were identified as having a significant change in abundance in HGT as in Figure 6.

## 3.3 Influence of methanol treatments on leaf physiology and LC-MS/MS metabolites ‗

In order to assess the effect of methanol treatment on temperature acclimation, we then compared leaf physiology data from plants treated with 9 mM and 27 mM methanol with control 0 mM methanol saplings, as discussed previously in section 3.1 (**Figures 1 – 4**). Regular soil watering with 9 mM and 27 mM solutions of methanol did not result in large enhancements to $P_n$ in plants at either LGT or HGT, relative to control plants that were not treated with methanol (**Figure 1**).

Similarly, changes due to the methanol treatments could not be detected $g_s$ and E. For each of the applied methanol concentrations (0, 9, 27 mM), the % change in the mean values were calculated between the LGT and the HGT. This analysis did not reveal any statistically significant trend in the HGT suppressions of $P_n$, E, and $g_s$ due to the methanol treatments (**Figure 1**). Across control and methanol treatments, the range of HGT suppression was similar for $P_n$ (50-52%), E (52-56%), and $g_s$ (58-61%). In addition, methanol treatments did not result in large changes to photochemical parameters of photosynthesis in plants at either LGT or HGT relative to control 0 mM methanol plants (**Figure 2**). As with the gas exchange parameters, small methanol-driven changes to ETR, Fv'/Fm', and qp may have occurred, but were not detectable due to the high variability from each of the six individuals within each treatment. However, when the % change in the mean values were calculated between the LGT and HGT plants at each methanol concentration, a non-significant negative trend with methanol concentration in the mean values was observed (**Figure 2**), with the largest % change observed under 27 mM methanol and the lowest with control 0 mM plants. Thus, contrary to **H2**, methanol treatments appeared to negatively impact ETR, Fv'/Fm', and $q_p$ as detected by an enhanced suppression of ETR, Fv'/Fm', and $q_p$ by the high growth temperature. Under the control water treatment, mean values of ETR, Fv'/Fm', and $q_p$ decreased by 44% between LGT and HGT plants. Despite failing statistical significance tests, under methanol treatment the HGT further suppressed the mean values of ETR, Fv'/Fm', and $q_p$ up to 48% (**Figure 2**). However, methanol treatments appeared to reduce the suppression of the mean values of leaf dark respiration ($R_d$) by the high growth temperature (36.8% suppression in water controls compared with 30.8-35% suppression in the methanol treatments). Likewise, methanol treatments appeared

to reduce the suppression of the mean values of estimates of photorespiration ($R_p$) by the high growth temperature (93.7% suppression in water controls compared with 56-62% suppression in the methanol treatments). However, given the high variability of responses in each treatment, the differences were not statistically significant (**Figure 3**).
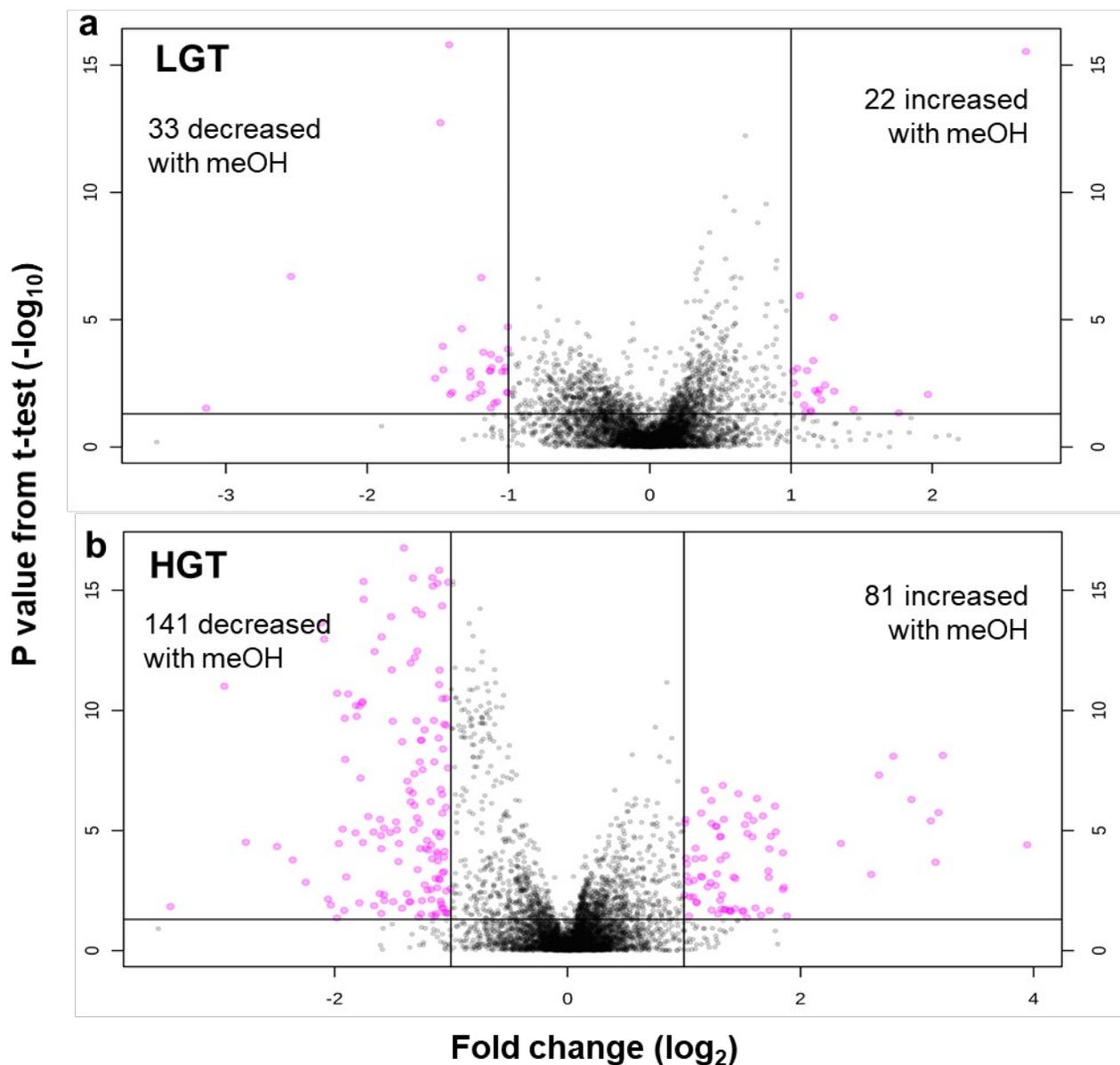
**Figure 7**: Volcano plot showing growth methanol-induced differences in extracted leaf compound abundances (LC-MS positive mode). Compounds that have a greater than $\pm$ 2-fold abundance change (x-axis) that is statistically significant ($p<0.05$, t-test; y axis) between LGT (**a**) and HGT (**b**) plants at 9 mM and 27 mM methanol are shown in pink. The number of significant compounds that decreased in abundance with methanol treatment is indicated on the left side of the plot, and

the number of compounds significantly increased with methanol treatment is indicated on the right side.

A small number of extracted leaf tissue metabolites (55 out of 10,015) showed significantly altered abundances under LGT and methanol treatment relative to water controls, and this greatly increased in compound number (222) at the HGT. At the LGT, 33 compounds decreased abundance with methanol, and 22 compounds increased in abundance with methanol (**Figure 7a**). There were a greater number of compounds showing a significant methanol-induced change in the HGT (**Figure 7b**), including 141 compounds that decreased with methanol and 81 compounds that increased. Interestingly, the compounds that changed in abundance in the methanol treatment were largely distinct from those that changed due to the HGT (**Figure 8**). Moreover, compounds that changed in abundance with methanol treatment at the LGT were largely distinct from compounds that changed in abundance with methanol at the HGT (**Figure 8** and **supplementary table 1**). Importantly, many compounds that decreased under HGT with water control (0 mM methanol), increased with methanol treatment at HGT. For instance, a compound tentatively identified as a flavonoid-glucuronide showed a -3.79 $\log_2$ fold change under HGT but increased by 3.22 $\log_2$ fold change under HGT in the presence of methanol (see **supplementary table 1** and **Table 4**). In addition, three compounds involved in lipid metabolism showed a decrease in abundance under HGT, and an increase at HGT with methanol treatment. As a final example, four compounds tentatively identified to be involved in secondary metabolism and two involved in flavonoid metabolic pathways showed this effect where a suppression in abundance at the HGT was reversed to increased abundances in the presence of methanol (**supplementary table 1**).
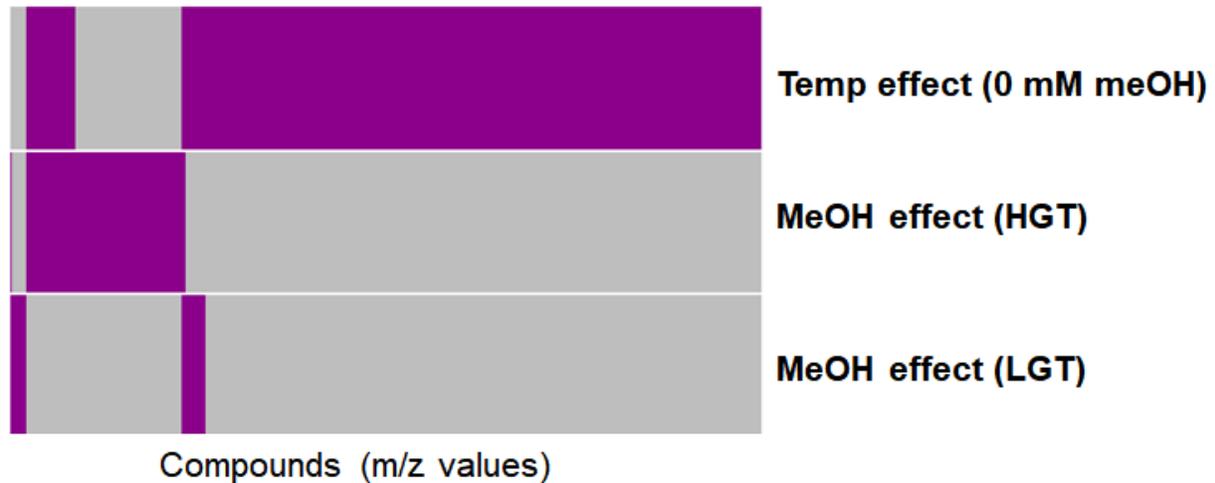
**Figure 8**: Heatmap of compounds that show a significant temperature or methanol effect. Magenta represents compounds that show a significant effect, a +/- 2-fold change in abundance, p<0.05 t-test, grey signifies no significant effect. The 1034 compounds identified in figure 6 are included in this plot, with 867 significant compounds represented for temperature effect, 222 for meOH effect at HGT and 55 for meOH effect at LGT. The m/z values range from 77 to 707. Compounds are grouped according to methanol or temperature effect.

## 4. **Discussion**

### 4.1 Response of leaf gas exchange and photosynthesis to HGT

Ongoing and predicted increases in surface temperatures beyond the optimal for plant metabolism can have strong negative impacts on plant productivity. Understanding the biochemical and physiological mechanisms behind plant thermal acclimation to high temperature is critical to improve our predictive understanding of how managed and natural forested ecosystems will shift their carbon metabolism and water usage including changes to net primary productivity and transpiration. Of

particular interest in the study of temperature acclimation of primary carbon metabolism are Poplars (*Populus spp.*), which are fast growing trees widely used for landscape, agriculture, phytoremediation, soil carbon sequestration, reduction in sediment run-off, improvement in soil quality, and habitat for wildlife[47]. In addition, poplar plantations are utilized for wood, composite biomaterials, and as a bioenergy feedstock assisted by genetic engineering strategies that target cell wall recalcitrance[48]. Poplar species are generally considered drought tolerant, although this tolerance and ability to acclimate varies across species[49]. In this study, we tested two hypotheses related to temperature acclimation in *P. trichocarpa*, and evaluated them using a unique combination of leaf gas exchange, chlorophyll fluorescence, and extractable leaf metabolite concentrations. In **H1**, we hypothesized that $g_s$ will be down regulated at high growth temperatures and this will lead to a suppression in E, $P_n$, and due to its tight metabolic connections with photosynthesis, also dark respiration ($R_d$) and photorespiration ($R_p$). However, the optimum temperature of ETR will be stimulated as well as the emissions of isoprene through the utilization of products of the light reactions[17]. We also hypothesized (**H2**) that an important metabolic role of the methanol-initiated $C_1$ pathway occurs during high temperature stress in $C_3$ plants. Specifically, we hypothesized that for *P. trichocarpa* saplings grown at a high growth temperature, methanol-treated plants will show increased thermotolerance of photosynthesis displayed by higher rates of $P_n$ and photochemical parameters of the light reactions including ETR, Fv'/Fm', and $q_p$. Moreover, due to $CO_2$ production via the $C_1$ pathway, methanol-treated plants are anticipated to have suppressed rates of photorespiration ($R_p$) and enhanced dark respiration ($R_D$). Finally, methanol-treated plants will have higher leaf

concentrations of photosynthetic products including sugars, fatty acids, isoprenoids, etc.

Our observations directly support **H1** and are largely consistent with the results of a previous studies on temperature acclimation in poplar[20,50,51]. Hybrid poplar clones (*P. maximowiczii x P. nigra and P. maximowiczii x P. balsamifera*)[50] and *P. tremula* saplings[51] grown at an elevated temperature showed an increase in $T_{Opt}$ and acclimation of $R_d$ [50]. Equally, *P. euramericana* saplings at the same growth temperatures used in the present study (HGT, 35°C and LGT, 25°C), which showed a considerable downward acclimation of $P_n$, $g_s$, and both dark ($R_d$) and light respiration ($R_l$)[20]. The only apparent difference is the finding from our study that mean leaf isoprene emissions from *P. trichocarpa*, determined at a leaf temperature of 40°C, is higher in HGT plants than LGT. In contrast, the study on *P. euramericana*[20] showed suppressed isoprene emissions in HGT plants relative to LGT plants at temperatures above 25°C. One potential explanation for our observation of increased isoprene emissions at high leaf temperature (40°C) in the present study on *P. trichocarpa* is the stimulation of the optimum leaf temperature of ETR in HGT plants relative to LGT plants. HGT plants showed an average upward acclimation of the optimum temperature by 3.0°C (LGT: 35.7°C versus HGT: 38.7°C), with values observed for HGT plants up to 40.6°C. This finding is consistent with previous observations of a substantial increase in the thermal optimum of the maximum rate of photosynthetic electron transport ($J_{max}$)[12] during temperature acclimation and a stimulation of both isoprene emissions and ETR rates as a key mechanism of thermotolerance[17]. Isoprene emissions have been demonstrated to positively correlate with leaf temperature[52] and are directly linked to photosynthesis through both carbon skeletons and the consumption of photosynthetic ATP/NADPH, which can be in

"excess" during partial stomatal closure at high temperatures. This process is thought to reduce the over-reduction of the chloroplast and consequently attenuate photo-oxidative damage[53] . Thus, isoprene emissions are regularly observed to increase, and therefore decouple, from $P_n$ and $g_s$ during high temperatures such as observed during heatwave conditions in black locust trees[54] and heat stressed *P. deltoides x nigra*[55]. Recently, this was explained by the tight coupling of ETR and isoprene emissions, where ETR is known to have a higher temperature optimum than $P_n$ and $g_s$[17]. The results support a view that despite of a suppression of its magnitude relative to LGT plants, an enhancement of the optimum temperature of ETR and the activity of pathways that utilize the end products of ETR (ATP and NADPH) including isoprene biosynthesis, represents a rapid thermal acclimation mechanism for *P. trichocarpa* and potentially other poplar species.

The co-suppression of both $P_n$ and $R_d$ by a similar magnitude by the HGT (51% and 37%, respectively) is consistent with a recent synthesis study on model and observations spanning all terrestrial biomes that concluded basal rates of $V_{cmax}$ and leaf mitochondrial 'dark' respiration ($R_d$), assessed at 25°C, decrease by ~4.4% per °C increase in growth temperature[56]. Thus, given the 10°C increase in growth temperature from LGT to HGT conditions in the present study, a ~44% decrease in and $R_d$ can be expected according to the synthesis study[56], when assessed at 25°C. Although we assessed $R_d$ at 30°C leaf temperature, this compares reasonably well with the observed 37% average decrease observed in the current study on potted *P. trichocarpa* saplings. These findings support the emerging view of strong dependence of respiration on photosynthesis substrate supply and demand for respiratory products[56].

Estimated photorespiration rates were lower in HGT plants than LGT plants; this may be attributed to the environmental conditions that we used to carry out our assessments. As we carried out our assessment at 30°C, a lower temperature than the growth temperature of HGT plants, it is possible that HGT plants had acclimated sufficiently that Rubisco specificity for $CO_2$ was higher in the HGT plants. This could potentially lead to a lower inhibition of photosynthesis at 30°C compared to LGT plants. In addition, decreased dark-acclimated Fv/Fm, ETR, $q_p$ and Fv'/Fm', along with decreased $P_n$ and $R_p$ indicate reduced photosynthetic capacity in HGT plants compared to LGT plants.

To summarize, we extended the analysis of gas exchange of thermal acclimation of *P. trichocarpa* by simultaneously quantifying key parameters of the light reactions of photosynthesis. Our observations suggest that reduced stomatal conductance ($g_s$) at the HGT is associated with the suppression of gas exchange including $P_n$ and E and led to associated decreases in photochemical parameters of photosynthesis including electron transport rates (ETR), quantum yield of PSII in the light (Fv'/Fm'), and photochemical quenching ($q_p$). Nonetheless, this was associated with the upregulation of energy dissipating processes in HGT plants including non-photochemical quenching (NPQt) and leaf isoprene emissions at 40°C. The increase in $NPQ_t$ occurs through regulation of the light harvesting system as a photo-protective mechanism, and results in heat production rather than over-reduction of the chloroplast, formation of reaction oxygen species like singlet oxygen and hydrogen peroxide[57].

**4.2 Response of leaf gas exchange and photosynthesis to methanol**

Although the HGT treatment caused large impacts on gas exchange and the photochemical parameters of photosynthesis, relative to the LGT, methanol effects were less clear. This could be in part due to the relatively large variation observed among treatments, along with the relatively small sample size of six individuals per treatment, as demonstrated in **Figure 5a,b**. This relatively large biological variation may be related to natural variability including differences in leaf developmental stages or to variations in the environmental conditions each leaf was exposed to (e.g. light level), thereby masking any effects that methanol treatment may have on gas exchange and the photochemical parameters of photosynthesis. Thus, we were unable to conclusively support or reject **H2** with our experiment, but several suggestions can be made from the data. However, it should be noted that we were unable to verify that the potted seedlings actively took up the methanol solutions into their transpiration stream, as methylotrophic bacteria and other microorganisms are known to be highly abundant in soils with methylotrophy proteins can be among the most abundant proteins in the proteome[58]. Therefore, microbial methylotrophy in the soils may have effectively competed against the roots for methanol solution uptake in the soil. Future experiments should therefore verify the successful delivery of methanol solutions to soils via emission measurements of methanol from the foliage; methanol emissions from treated plants should be substantially higher than in water fed controls. An alternative method would be to supply methanol via a spray directly onto leaves rather than delivery to the soil. For instance, foliar application of methanol has been shown to ameliorate salinity stress in *Lavandula stoechas*[59] and soybean[60], and drought stress in *Phaseolus vulgaris*[61].

Contrary to **H2**, methanol treatments appeared to negatively impact ETR, Fv'/Fm', and $q_p$ as detected by an enhanced suppression of ETR, Fv'/Fm', and $q_p$ by the high growth temperature as a function of methanol concentrations (% change LGT→HGT, **Figure 2**). Although the trend was not statistically significant, the results are in line with studies on the toxic effects of formaldehyde on photosynthesis, the main product of methanol oxidation via the $C_1$ pathway. Formaldehyde is highly reactive with many biopolymers and leaf chlorosis and bleach with a complete loss of photosynthetic carbon assimilation has been observed under high formaldehyde levels. Under moderately high levels, Arabidopsis seedlings exposed to 2-4 mM formaldehyde were observed to reduce total chlorophyll content, $P_n$, and the expression of numerous photosynthesis related genes[62]. Moreover, as formaldehyde is detoxified in the $C_1$ pathway to formate via formaldehyde dehydrogenase (FALDH), transgenic tobacco overexpressing FALDH conferred tolerance up to formaldehyde concentrations of 6 mM[63]. Relative to wild type, the transgenic tobacco lines under formaldehyde stress produced higher biomass, total chlorophyll, protein, and soluble sugar content, as well as reduced levels of oxidative stress detected by lower levels of lipid peroxidation and $H_2O_2$ as compared with the wild-type tobacco. Thus, future studies on the role of methanol in temperature acclimation could take advantage of transgenic plants overexpressing FALDH and demonstrated to have enhanced tolerance to formaldehyde stress.

Exogenous methanol was hypothesized (**H2**) to play a protective role during heat stress through its production of $CO_2$ via the $C_1$ pathway. Under the levels of exogenously supplied methanol added to the soil in this study (0, 9, 27 mM), a quantitatively significant internal plant source of $CO_2$ was hypothesized that becomes important when atmospheric $CO_2$ uptake is limited due to partial stomatal

closure at HGT. Methanol treatments appeared to reduce the suppression of the mean values of leaf dark respiration ($R_d$). When the effect of methanol additions on the % change of $R_d$ between LGT and HGT treatments was calculated (**Figure 3**), water controls showed a 36.8% suppression compared with 30.8-35% suppression in the methanol treatments). Likewise, methanol treatments appeared to reduce the suppression of the mean values of estimates of photorespiration in the light ($R_p$) by the high growth temperature (93.7% suppression in water controls compared with 56-62% suppression in the methanol treatments). Given that methanol supplied to the transpiration stream in plants can lead to enhanced $CO_2$ production via formate oxidation[36], a reduced suppression of $R_d$ and $R_p$ in HGT plants relative to LGT plants could be expected. This is because methanol-treated HGT plants are expected to show an enhanced non-mitochondrial "respiratory" source of $CO_2$. However, these average % changes were not statistically significant due to the high variability within the temperature and methanol experimental treatments. Thus, while conclusive evidence was not obtained, the results are consistent with the view that exogenous methanol both impairs photochemistry of the light reactions at HGT (potentially by formaldehyde toxicity), and stimulates photosynthesis and dark respiration at HGT through formate oxidation to $CO_2$.

**4.3 Metabolomic response of poplar to HGT and methanol**

Although most studies focus on one or the other, in this study we collected both leaf physiological and metabolomic data in parallel over the two-month experimental period. LC-MS metabolomics data was collected in order to allow for insight into the relative responses of leaf extractable metabolites to both increased growth temperature and methanol additions to soils (**H1**). We were only able to

obtain putative identities, often to the compound class level, of 110 out of 867 features that showed a significant response to HGT or methanol treatment. Metabolomics data revealed alterations in flavonoid abundances with temperature stress. Flavonoids serve as effective antioxidants and genes involved in the flavonoid biosynthesis pathway have been implicated in response to heat stress[64]. A number of anthocyanin compounds, a class of highly pigmented flavonoid compounds, were reported to have been significantly modified in abundance by the HGT, with their biosynthesis previously demonstrated to be suppressed under HGT in Arabidopsis[65], grapevine berries[66] and apple fruit[67]. Thus, flavonoids are considered to play a central role in acclimation to heat stress, via ROS homeostasis regulation[68]. The observed decrease in abundance of lipid compounds and metabolism at HGT could be due in part to the increase in lipid peroxidation which occurs at high temperatures[69], as well as changes in the expression of genes relating to lipid metabolism.

Importantly, our analysis revealed that high growth temperature and methanol treatments have largely distinct patterns of impacts on metabolites. Compounds that were altered in abundance in the methanol treatment were largely distinct from those that changed due to the HGT. Moreover, compounds that changed in abundance with methanol treatment at the LGT were largely distinct from compounds that changed in abundance with methanol at the HGT. Therefore, distinct metabolic 'signatures' can be attributed to the high temperature treatment as well as methanol treatment at both the low and high temperatures. Moreover, a number of metabolites that decreased under HGT, increased with the addition of methanol at HGT, or vice versa. This suggests that methanol may have a protective effect against heat stress in some metabolic pathways. However, we were unable to

obtain definitive identities for many of these metabolites. Further in-depth metabolomic studies would be valuable to fully understand the impact of HGT and exogenous methanol on plant metabolism, particularly flavonoid biosynthesis pathways.

Gene expression can be modified by DNA methylation. DNA methylation patterns were altered throughout multiple generations of *Plantago lanceolata* grown under elevated $CO_2$[70]. Although we were unable to collect transcriptomics data, we speculate that the addition of methanol could provide the material for increased DNA methylation, thus affecting specific gene expression. Thus, future studies evaluating the role of exogenous methanol on poplar temperature acclimation should aim at collecting physiological, metabolomics, and transcriptomics data together. This is a great technical challenge and opportunity to advance our mechanistic understanding of the role of methanol metabolism in high temperature responses.

## Conclusion

Temperature acclimation of poplar trees is important to understand in the face of climate change-induced increase of surface temperatures and its corresponding impact on tree productivity for biofuel and bioproducts. *Populus trichocarpa* trees showed acclimation to high growth temperature, indicated by a suppression in carbon cycling and leaf water use, attributed to decreased stomatal conductance. Importantly, we coupled these physiological measurements to chlorophyll fluorescence and metabolomics data, providing a comprehensive insight into temperature acclimation in this important biofuel species. We found large

physiological and biochemical impacts of high growth temperature on poplar seedlings leaf gas exchange and photochemistry and highlight the enhancement of the optimum temperature of ETR as a rapid thermal acclimation mechanism. Although application of methanol has been suggested to mitigate high temperature stress, we were unable to conclusively demonstrate this in our study. However, metabolomics analysis revealed a significant number of metabolites that altered under HGT, and some of these changes were reversed with methanol, suggesting a potential protective role of methanol against high temperatures in some metabolic pathways.

## 5. <u>Acknowledgments</u>

## 6. <u>Funding sources</u>

## 7. <u>Author contributions</u>

The experiments were designed and carried out, and the manuscript written through contributions of all authors. All authors have given approval to the final version of the manuscript.

## 8. <u>Abbreviations</u>

E, transpiration; ETR, electron transport rate; Fv'/Fm', quantum yield of PSII in the light; $g_s$, stomatal conductance; HGT, high growth temperature; $J_{max}$ , maximum rate of photosynthetic electron transport; LC-MS, liquid chromatography mass spectrometry; LGT, low growth temperature; meOH, methanol;  $NPQ_t$, non-photochemical quenching of excitons in photosystem-II-associated antenna complexes; $P_n$, net photosynthesis; $q_p$, photochemical quenching; $R_D$, dark respiration; $R_p$, photorespiration; $V_{cmax}$, thermal optimum of photosynthetic capacity

## 9. <u>Supporting information</u>

**Table S1: Leaf metabolomics data based on LC-MS**: All features that showed a

significant (p>0.05, t-test) +/- 2-fold log change in abundance are included. The m/z

values, retention times, ID, log2fold change and p value (for temperature and

methanol effects) are included.

## 10. <u>References</u>

(1)     Newman, B. D.; Wilcox, B. P.; Archer, S. R.; Breshears, D. D.; Dahm, C. N.;
        Duffy, C. J.; McDowell, N. G.; Phillips, F. M.; Scanlon, B. R.; Vivoni, E. R.
        Ecohydrology of water-limited environments: A scientific vision. *Water Resour.
        Res.* **2006**, *42*.
(2)     Slot, M.; Garcia, M. N.; Winter, K. Temperature response of CO2 exchange in
        three tropical tree species. *Funct. Plant Biol.* **2016**, *43*, 468–478.
(3)     Barigah, T. S.; Charrier, O.; Douris, M.; Bonhomme, M.; Herbette, S.; Améglio,
        T.; Fichot, R.; Brignolas, F.; Cochard, H. Water stress-induced xylem hydraulic
        failure is a causal factor of tree mortality in beech and poplar. *Ann. Bot.*
        **2013**, *112*, 1431–1437.
(4)     Zhao, M.; Running, S. W. Drought-induced reduction in global terrestrial net
        primary production from 2000 through 2009. *Science* **2010**, *329*, 940–943.
(5)     Pfeifer, E. M.; Hicke, J. A.; Meddens, A. J. H. Observations and modeling of
        aboveground tree carbon stocks and fluxes following a bark beetle outbreak
        in the western United States. *Glob. Change Biol.* **2011**, *17*, 339–350.
(6)     Brienen, R. J. W.; Phillips, O. L.; Feldpausch, T. R.; Gloor, E.; Baker, T. R.; Lloyd,
        J.; Lopez-Gonzalez, G.; Monteagudo-Mendoza, A.; Malhi, Y.; Lewis, S. L.; et al.
        Long-term decline of the Amazon carbon sink. *Nature* **2015**, *519*, 344–348.
(7)     Tuskan, G. A.; DiFazio, S. P.; Teichmann, T. Poplar genomics is getting
        popular: the impact of the poplar genome project on tree research. *Plant Biol.
        (Stuttg.)* **2004**, *6*, 2–4.
(8)     Mortimer, J. C. Plant synthetic biology could drive a revolution in biofuels and
        medicine. *Exp. Biol. Med.* **2019**, *244*, 323–331.
(9)     Long, S. P. Modification of the response of photosynthetic productivity to
        rising temperature by atmospheric CO2 concentrations: Has its importance
        been underestimated? *Plant Cell Environ.* **1991**, *14*, 729–739.
(10)    Jardine, K.; Chambers, J.; Alves, E. G.; Teixeira, A.; Garcia, S.; Holm, J.;
        Higuchi, N.; Manzi, A.; Abrell, L.; Fuentes, J. D.; et al. Dynamic balancing of
        isoprene carbon sources reflects photosynthetic and photorespiratory
        responses to temperature stress. *Plant Physiol.* **2014**, *166*, 2051–2064.
(11)    Hikosaka, K.; Ishikawa, K.; Borjigidai, A.; Muller, O.; Onoda, Y. Temperature
        acclimation of photosynthesis: mechanisms involved in the changes in

temperature dependence of photosynthetic rate. *J. Exp. Bot.* **2006**, *57*, 291–302.

(12)  Kumarathunge, D. P.; Medlyn, B. E.; Drake, J. E.; Tjoelker, M. G.; Aspinwall, M. J.; Battaglia, M.; Cano, F. J.; Carter, K. R.; Cavaleri, M. A.; Cernusak, L. A.; et al. Acclimation and adaptation components of the temperature dependence of plant photosynthesis at the global scale. *New Phytol.* **2019**, *222*, 768–784.

(13)  Berry, J.; Bjorkman, O. Photosynthetic response and adaptation to temperature in higher plants. *Annu. Rev. Plant Physiol.* **1980**, *31*, 491–543.

(14)  Way, D. A.; Yamori, W. Thermal acclimation of photosynthesis: on the importance of adjusting our definitions and accounting for thermal acclimation of respiration. *Photosyn Res* **2014**, *119*, 89–100.

(15)  Slot, M.; Winter, K. In situ temperature response of photosynthesis of 42 tree and liana species in the canopy of two Panamanian lowland tropical forests with contrasting rainfall regimes. *New Phytol.* **2017**, *214*, 1103–1117.

(16)  Lloyd, J.; Farquhar, G. D. Effects of rising temperatures and [CO2] on the physiology of tropical forest trees. *Philos. Trans. R. Soc. Lond. B, Biol. Sci.* **2008**, *363*, 1811–1817.

(17)  Rodrigues, T. B.; Baker, C. R.; Walker, A. P.; McDowell, N.; Rogers, A.; Higuchi, N.; Chambers, J. Q.; Jardine, K. J. Stimulation of isoprene emissions and electron transport rates as key mechanisms of thermal tolerance in the tropical species Vismia guianensis. *Glob. Change Biol.* **2020**, *26*, 5928–5941.

(18)  Zait, Y.; Shtein, I.; Schwartz, A. Long-term acclimation to drought, salinity and temperature in the thermophilic tree Ziziphus spina-christi: revealing different tradeoffs between mesophyll and stomatal conductance. *Tree Physiol.* **2019**, *39*, 701–716.

(19)  Smith, N. G.; McNellis, R.; Dukes, J. S. No acclimation: instantaneous responses to temperature maintain homeostatic photosynthetic rates under experimental warming across a precipitation gradient in Ulmus americana. *AoB Plants* **2020**, *12*, plaa027.

(20)  Fares, S.; Mahmood, T.; Liu, S.; Loreto, F.; Centritto, M. Influence of growth temperature and measuring temperature on isoprene emission, diffusive limitations of photosynthesis and respiration in hybrid poplars. *Atmos. Environ.* **2011**, *45*, 155–161.

(21)  Ruehr, N. K.; Gast, A.; Weber, C.; Daub, B.; Arneth, A. Water availability as dominant control of heat stress responses in two contrasting tree species. *Tree Physiol.* **2016**, *36*, 164–178.

(22)  Paupière, M. J.; Tikunov, Y.; Schleiff, E.; Bovy, A.; Fragkostefanakis, S. Reprogramming of tomato leaf metabolome by the activity of heat stress transcription factor hsfb1. *Front. Plant Sci.* **2020**, *11*, 610599.

(23)  Hancock, R. D.; Morris, W. L.; Ducreux, L. J. M.; Morris, J. A.; Usman, M.; Verrall, S. R.; Fuller, J.; Simpson, C. G.; Zhang, R.; Hedley, P. E.; et al. Physiological, biochemical and molecular responses of the potato (*Solanum tuberosum* L.) plant to moderately elevated temperature. *Plant Cell Environ.* **2014**, *37*, 439–450.

(24) Wang, L.; Ma, K.-B.; Lu, Z.-G.; Ren, S.-X.; Jiang, H.-R.; Cui, J.-W.; Chen, G.; Teng, N.-J.; Lam, H.-M.; Jin, B. Differential physiological, transcriptomic and metabolomic responses of Arabidopsis leaves under prolonged warming and heat shock. *BMC Plant Biol.* **2020**, *20*, 86.

(25) Liu, B.; Zhang, L.; Rusalepp, L.; Kaurilind, E.; Sulaiman, H. Y.; Püssa, T.; Niinemets, Ü. Heat-priming improved heat tolerance of photosynthesis, enhanced terpenoid and benzenoid emission and phenolics accumulation in Achillea millefolium. *Plant Cell Environ.* **2020**.

(26) Eriksen, R. L.; Padgitt-Cobb, L. K.; Townsend, M. S.; Henning, J. A. Gene expression for secondary metabolite biosynthesis in hop (Humulus lupulus L.) leaf lupulin glands exposed to heat and low-water stress. *Sci. Rep.* **2021**, *11*, 5138.

(27) Shen, J.; Zhang, D.; Zhou, L.; Zhang, X.; Liao, J.; Duan, Y.; Wen, B.; Ma, Y.; Wang, Y.; Fang, W.; et al. Transcriptomic and metabolomic profiling of Camellia sinensis L. cv. "Suchazao" exposed to temperature stresses reveals modification in protein synthesis and photosynthetic and anthocyanin biosynthetic pathways. *Tree Physiol.* **2019**, *39*, 1583–1599.

(28) Feldman, D. R.; Collins, W. D.; Gero, P. J.; Torn, M. S.; Mlawer, E. J.; Shippert, T. R. Observational determination of surface radiative forcing by CO2 from 2000 to 2010. *Nature* **2015**, *519*, 339–343.

(29) Garcia, S.; Jardine, K.; Souza, V.; Souza, R.; Duvoisin Junior, S.; Gonçalves, J. Reassimilation of Leaf Internal CO2 Contributes to Isoprene Emission in the Neotropical Species Inga edulis Mart. *Forests* **2019**, *10*, 472.

(30) Doman, N. G.; Romanova, A. K. Transformations of labeled formic acid, formaldehyde, methanol, & CO(2) absorbed by bean & barley leaves from air. *Plant Physiol.* **1962**, *37*, 833–840.

(31) Dewhirst, R. A.; Afseth, C. A.; Castanha, C.; Mortimer, J. C.; Jardine, K. J. Cell wall O-acetyl and methyl esterification patterns of leaves reflected in atmospheric emission signatures of acetic acid and methanol. *PLoS One* **2020**, *15*, e0227591.

(32) Voragen, A. G. J.; Schols, H. A.; Pilnik, W. Determination of the degree of methylation and acetylation of pectins by h.p.l.c. *Food Hydrocoll.* **1986**, *1*, 65–70.

(33) Harley, P.; Greenberg, J.; Niinemets, Ü. Environmental controls over methanol emission from leaves. *Biogeosciences* **2007**, *4*, 1083–1099.

(34) Jacob, D. J. Global budget of methanol: Constraints from atmospheric observations. *J. Geophys. Res.* **2005**, *110*.

(35) Song, Z.-B.; Xiao, S.-Q.; You, L.; Wang, S.-S.; Tan, H.; Li, K.-Z.; Chen, L.-M. C1 metabolism and the Calvin cycle function simultaneously and independently during HCHO metabolism and detoxification in Arabidopsis thaliana treated with HCHO solutions. *Plant Cell Environ.* **2013**, *36*, 1490–1506.

(36) Jardine, K. J.; Fernandes de Souza, V.; Oikawa, P.; Higuchi, N.; Bill, M.; Porras, R.; Niinemets, Ü.; Chambers, J. Q. Integration of $C_1$ and $C_2$ metabolism in trees. *Int. J. Mol. Sci.* **2017**, *18*, 2045.

(37) Nonomura, A. M.; Benson, A. A. The path of carbon in photosynthesis: improved crop yields with methanol. *Proc. Natl. Acad. Sci. USA* **1992**, *89*, 9794–9798.

(38) McGiffen, M. E.; Manthey, J. A. The role of methanol in promoting plant growth: A current evaluation. *horts.* **1996**, *31*, 1092–1096.

(39) Rowe, R. N.; Farr, D. J.; Richards, B. A. J. Effects of foliar and root applications of methanol or ethanol on the growth of tomato plants ( *Lycopersicon esculentum* Mill). *N. Z. J. Crop Hortic. Sci.* **1994**, *22*, 335–337.

(40) McGiffen, M. E.; Green, R. L.; Manthey, J. A.; Faber, B. A.; Downer, A. J.; Sakovich, N. J.; Aguiar, J. Field tests of methanol as a crop yield enhancer. *horts.* **1995**, *30*, 1225–1228.

(41) Dewhirst, R. A.; Lei, J.; Afseth, C. A.; Castanha, C.; Wistrom, C. M.; Mortimer, J. C.; Jardine, K. J. Are Methanol-Derived Foliar Methyl Acetate Emissions a Tracer of Acetate-Mediated Drought Survival in Plants? *Plants* **2021**, *10*.

(42) Baker, N. R.; Rosenqvist, E. Applications of chlorophyll fluorescence can improve crop production strategies: an examination of future possibilities. *J. Exp. Bot.* **2004**, *55*, 1607–1621.

(43) Earl, H. J.; Tollenaar, M. Relationship between thylakoid electron transport and photosynthetic CO2 uptake in leaves of three maize (Zea mays L.) hybrids. *Photosyn Res* **1998**, *58*, 24–257.

(44) Katajamaa, M.; Miettinen, J.; Oresic, M. MZmine: toolbox for processing and visualization of mass spectrometry based molecular profile data. *Bioinformatics* **2006**, *22*, 634–636.

(45) Xia, J.; Wishart, D. S. Using metaboanalyst 3.0 for comprehensive metabolomics data analysis. *Curr Protoc Bioinformatics* **2016**, *55*, 14.10.1–14.10.91.

(46) Tietz, S.; Hall, C. C.; Cruz, J. A.; Kramer, D. M. NPQ(T) : a chlorophyll fluorescence parameter for rapid estimation and imaging of non-photochemical quenching of excitons in photosystem-II-associated antenna complexes. *Plant Cell Environ.* **2017**, *40*, 1243–1255.

(47) Stanton, B.; Eaton, J.; Johnson, J.; Rice, D. Hybrid poplar in the Pacific Northwest: the effects of market-driven management. *J. For.* **2002**, *100*, 28–33.

(48) Bryant, N. D.; Pu, Y.; Tschaplinski, T. J.; Tuskan, G. A.; Muchero, W.; Kalluri, U. C.; Yoo, C. G.; Ragauskas, A. J. Transgenic poplar designed for biofuels. *Trends Plant Sci.* **2020**, *25*, 881–896.

(49) Jia, H.; Wang, L.; Li, J.; Sun, P.; Lu, M.; Hu, J. Comparative metabolomics analysis reveals different metabolic responses to drought in tolerant and susceptible poplar species. *Physiol. Plant.* **2020**, *168*, 531–546.

(50) Benomar, L.; Moutaoufik, M. T.; Elferjani, R.; Isabel, N.; DesRochers, A.; El Guellab, A.; Khlifa, R.; Idrissi Hassania, L. A. Thermal acclimation of photosynthetic activity and RuBisCO content in two hybrid poplar clones. *PLoS One* **2019**, *14*, e0206021.

(51) Dai, L.; Xu, Y.; Harmens, H.; Duan, H.; Feng, Z.; Hayes, F.; Sharps, K.; Radbourne, A.; Tarvainen, L. Reduced photosynthetic thermal acclimation capacity under elevated ozone in poplar (Populus tremula) saplings. *Glob. Change Biol.* **2021**.

(52) Singsaas, E. L.; Sharkey, T. D. The effects of high temperature on isoprene synthesis in oak leaves. *Plant Cell Environ.* **2000**, *23*, 751–757.

(53) Fini, A.; Brunetti, C.; Loreto, F.; Centritto, M.; Ferrini, F.; Tattini, M. Isoprene responses and functions in plants challenged by environmental pressures associated to climate change. *Front. Plant Sci.* **2017**, *8*, 1281.

(54) Bamberger, I.; Ruehr, N. K.; Schmitt, M.; Gast, A.; Wohlfahrt, G.; Arneth, A. Isoprene emission and photosynthesis during heatwaves and drought in black locust. *Biogeosciences* **2017**, *14*, 3649–3667.

(55) Urban, J.; Ingwers, M. W.; McGuire, M. A.; Teskey, R. O. Increase in leaf temperature opens stomata and decouples net photosynthesis from stomatal conductance in Pinus taeda and Populus deltoides x nigra. *J. Exp. Bot.* 20**17,** 68*,* 1757–1767.

(56) Wang, H.; Atkin, O. K.; Keenan, T. F.; Smith, N. G.; Wright, I. J.; Bloomfield, K. J.; Kattge, J.; Reich, P. B.; Prentice, I. C. Acclimation of leaf respiration consistent with optimal photosynthetic capacity. *Glob. Change Biol.* **2020**, *26*, 2573–2583.

(57) Müller, P.; Li, X. P.; Niyogi, K. K. Non-photochemical quenching. A response to excess light energy. *Plant Physiol.* **2001**, *125*, 1558–1566.

(58) Butterfield, C. N.; Li, Z.; Andeer, P. F.; Spaulding, S.; Thomas, B. C.; Singh, A.; Hettich, R. L.; Suttle, K. B.; Probst, A. J.; Tringe, S. G.; et al. Proteogenomic analyses indicate bacterial methylotrophy and archaeal heterotrophy are prevalent below the grass root zone. *PeerJ* **2016**, *4*, e2687.

(59) Valizadeh-Kamran, R.; Vojodi Mehrabani, L.; Pessarakli, M. Effects of foliar application of methanol on some physiological characteristics of *Lavandula stoechas* L. under NaCl salinity conditions. *J. Plant Nutr.* **2019**, *42*, 261–268.

(60) Wei, P.; Chen, D.; Jing, R.; Zhao, C.; Yu, B. Ameliorative effects of foliar methanol spraying on salt injury to soybean seedlings differing in salt tolerance. *Plant Growth Regul.* **2015**, *75*, 133–141.

(61) Armand, N.; Amiri, H.; Ismaili, A. Interaction of Methanol Spray and Water-Deficit Stress on Photosynthesis and Biochemical Characteristics of Phaseolus vulgaris L. cv. Sadry. *Photochem. Photobiol.* **2016**, *92*, 102–110.

(62) Wang, S.-S.; Song, Z.-B.; Sun, Z.; Zhang, J.; Mei, Y.; Nian, H.-J.; Li, K.-Z.; Chen, L.-M. Effects of Formaldehyde Stress on Physiological Characteristics and Gene Expression Associated with Photosynthesis in Arabidopsis thaliana. *Plant Mol. Biol. Rep.* **2012**, *30*, 1291–1302.

(63) Nian, H. J.; Meng, Q. C.; Cheng, Q.; Zhang, W.; Chen, L. M. The effects of overexpression of formaldehyde dehydrogenase gene from Brevibacillus brevis on the physiological characteristics of tobacco under formaldehyde stress. *Russ. J. Plant Physiol.* **2013**, *60*, 764–769.

(64) Su, P.; Jiang, C.; Qin, H.; Hu, R.; Feng, J.; Chang, J.; Yang, G.; He, G. Identification of Potential Genes Responsible for Thermotolerance in Wheat under High Temperature Stress. *Genes (Basel)* **2019**, *10*.

(65) Kim, S.; Hwang, G.; Lee, S.; Zhu, J.-Y.; Paik, I.; Nguyen, T. T.; Kim, J.; Oh, E. High Ambient Temperature Represses Anthocyanin Biosynthesis through Degradation of HY5. *Front. Plant Sci.* **2017**, *8*, 1787.

(66) Pastore, C.; Dal Santo, S.; Zenoni, S.; Movahed, N.; Allegro, G.; Valentini, G.; Filippetti, I.; Tornielli, G. B. Whole plant temperature manipulation affects flavonoid metabolism and the transcriptome of grapevine berries. *Front. Plant Sci.* **2017**, *8*, 929.

(67) Lin-Wang, K.; Micheletti, D.; Palmer, J.; Volz, R.; Lozano, L.; Espley, R.; Hellens, R. P.; Chagnè, D.; Rowan, D. D.; Troggio, M.; et al. High temperature reduces apple fruit colour via modulation of the anthocyanin regulatory complex. *Plant Cell Environ.* **2011**, *34*, 1176–1190.

(68) Muhlemann, J. K.; Younts, T. L. B.; Muday, G. K. Flavonols control pollen tube growth and integrity by regulating ROS homeostasis during high-temperature stress. *Proc. Natl. Acad. Sci. USA* **2018**, *115*, E11188–E11197.

(69) Narayanan, S.; Tamura, P. J.; Roth, M. R.; Prasad, P. V. V.; Welti, R. Wheat leaf lipids during heat stress: I. High day and night temperatures result in major lipid alterations. *Plant Cell Environ.* **2016**, *39*, 787–803.

(70) Saban, J. M.; Watson-Lazowski, A.; Chapman, M. A.; Taylor, G. The methylome is altered for plants in a high CO2 world: Insights into the response of a wild plant population to multigenerational exposure to elevated atmospheric [CO2 ]. *Glob. Change Biol.* **2020**, *26*, 6474–6492.
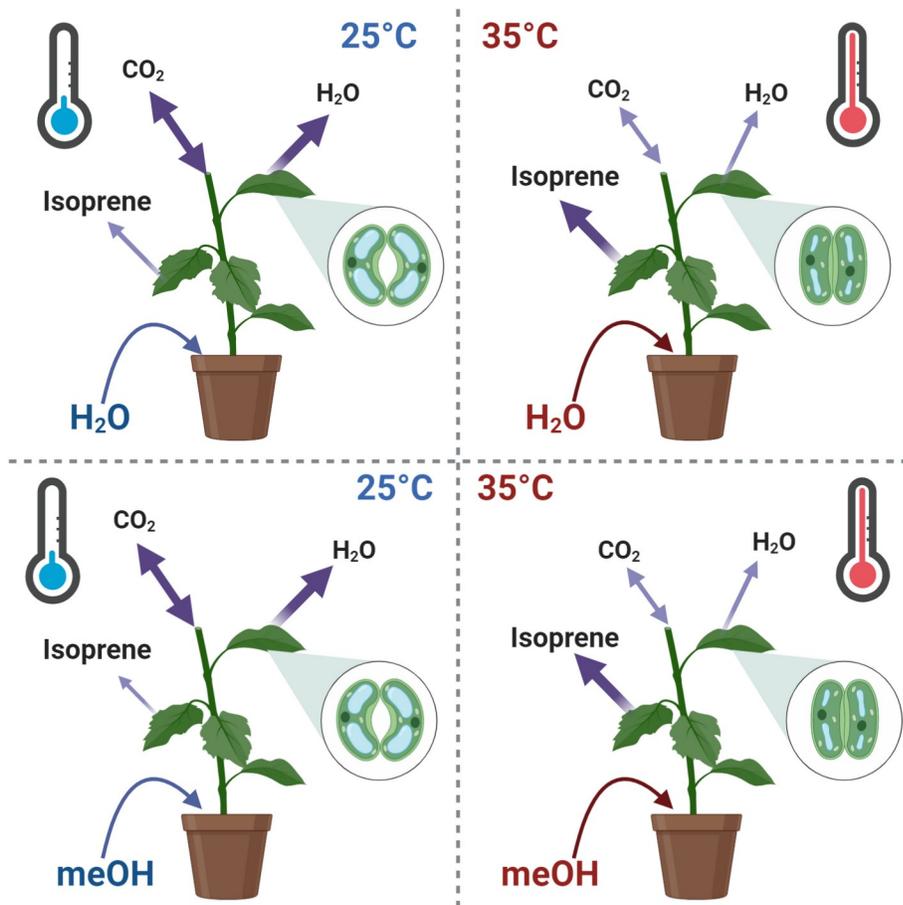
**TOC Graphic:** Summary of experimental treatments of potted poplar saplings including low and high growth temperature and water and methanol soil additions. Major fluxes relating to carbon cycling metabolism are indicated as well as stomatal conductance. The size of the arrows reflects the relative size of the fluxes.  This figure was created with BioRender (biorender.com)